Journal of Applied Polymer Science

WILEY

Applied Polymer SCIENCE

RESEARCH ARTICLE

Mathematical Modeling and Optimization of Poly(Ethylene Vinyl Alcohol) Film Thickness and Ethylene Composition Based on I-Optimal Design

Kowsar Rezvanian | Radhika Panickar | Faruk Soso | Vijaya Rangari

Department of Material Science and Engineering, College of Engineering, Tuskegee University, Tuskegee, Alabama, USA

Correspondence: Vijaya Rangari (vrangari@tuskegee.edu)

Received: 18 September 2024 | **Revised:** 11 January 2025 | **Accepted:** 22 January 2025

Funding: This study was supported by the Directorate for Education and Human Resources 1735971 and National Science Foundation 2132093.

Keywords: crystallization | glass transition | mechanical properties | thermal properties

ABSTRACT

Multilayer packaging is commonly used in the food industry to improve product preservation by combining materials with specific properties for optimal protection. Ethylene vinyl alcohol (EVOH) is highly valued for its barrier properties against air and moisture. The mechanical properties of EVOH films are influenced by both the ethylene content, which affects crystallinity and barrier performance, and the thickness of the EVOH layer, which affects the film's mechanical strength. This study develops mathematical models to explore the relationship between EVOH film thickness, ethylene content, and mechanical properties, such as tensile strength, elongation at break, and elastic modulus. Using RSM with I-optimal design, the optimal conditions for EVOH films are identified at a thickness of 0.03 mm and 48 mol% ethylene content. The model predicts values of 25.178% for elongation at break, 3077.865 MPa for elastic modulus, and 97.444 MPa for tensile strength. These predictions are validated through ANOVA, confirming the statistical significance of the model. Experimental results show achieved values of 27.119% for elongation, 3437.811 MPa for elastic modulus, and 107.308 MPa for tensile strength, demonstrating model accuracy. To further validate these findings, EVOH films are characterized by SEM, FTIR spectroscopy, and TGA, providing valuable insights into the structural and functional properties for food packaging.

1 | Introduction

Polymer-based packaging offers significant advantages over traditional materials like paper, aluminum, or glass due to its lightweight nature, lower energy requirements for production and adaptability to various applications. Many of these packages are designed as multilayer structures, combining various plastics in coextruded or laminated films. Each layer serves a specific purpose, such as enhancing mechanical strength or providing barrier protection, which improves the overall functionality and appearance of packaging. However, the use of multiple materials in these systems presents significant challenges for recycling. Ethylene vinyl alcohol (EVOH) is a crucial component in multilayer packaging due to its outstanding gas barrier properties, chemical resistance, and high transparency. Particularly effective with ethylene content below 38 mol%, EVOH prevents gas permeation, helping to preserve food quality and extend shelf life. EVOH's semicrystalline structure and strong inter- and intramolecular cohesive energy enable superior barrier performance against oxygen, nonpolar solvents, and food aromas under dry conditions, outperforming many other polymers [1, 2]. However, EVOH is moisture-sensitive, with its barrier and mechanical properties significantly diminishing under high relative humidity (RH) due to the disruption of cohesive energy. Despite this limitation, EVOH's versatility, especially in thin multilayer applications with thicknesses tailored for specific

uses, such as a few micrometers in food packaging or 50–100 μm in floor heating pipes, enhances the functionality and sustainability of food packaging systems, making it a valuable material in modern packaging technologies [3, 4].

The intrinsic characteristics of EVOH, including its chemical structure, crystallinity, glass transition temperature (*T*g), free volume, and thickness, play a critical role in its barrier and mechanical properties. These factors, particularly thickness, are key to determining the oxygen and moisture barrier performance of both single and multilayer film structures [5]. Thickness has an inverse relationship with oxygen gas transmission rate (O_2GTR) and water vapor permeability (PH_2O), with thicker layers offering improved barrier performance [6]. However, EVOH's sensitivity to moisture and its typical thin application limit its effectiveness as a water vapor barrier compared to materials like LDPE or PET, which are often used in thicker layers for better mechanical and barrier performance [7].

Film thickness has a distinct impact on mechanical properties and is a critical factor influencing the performance of both single-layer and multilayer films [8]. Therefore, to optimize EVOH's performance across diverse applications, it is crucial to understand the interplay between intrinsic and extrinsic factors. Similarly, a deep understanding of the mechanisms influencing the mechanical properties of plastic films is essential for driving advancements in scientific and technological applications. According to Scholtyssek et al. in multilayer films, when the PP/PS film thickness was reduced from 250 to 25 μm, the strain at break increased from 66% to 271% [9]. Additionally, the final properties of polymer films are influenced not only by film thickness and postprocessing but also by preparation conditions [10, 11]. In a study done by Cabedo et al. the mechanical properties of EVOH copolymers were analyzed under varying RH conditions. The research found that at low RH, mechanical properties are better, while at higher RH, water acts as a plasticizer, reducing performance [12]. Rouhi et al. investigated the effects of glycerol, bacterial cellulose nanocrystals (BCNCs), and boric acid concentrations on the mechanical properties of PVA-based films, using response surface methodology (RSM) and central composite rotatable design. Results indicated that the optimal conditions for maximum mechanical performance included specific concentrations of glycerol, BCNC, and boric acid, with the optimized films demonstrating improved ultimate tensile strength, elongation at break, and other mechanical properties [13]. Tafa et al. optimized starch-based edible films for food packaging using RSM, focusing on tef starch, agar, and glycerol concentrations [14]. Increasing glycerol reduced tensile strength, elastic modulus, and puncture force while improving elongation at break, whereas higher agar concentrations enhanced mechanical properties. The optimized formulation (5 g of tef starch, 0.4 g of agar, and 0.3% glycerol) produced films with superior tensile strength, elastic modulus, and puncture force. XRD and SEM analyses confirmed improved crystallinity and structural integrity. The study demonstrated that tef starch-based films with proper agar and glycerol levels could be a sustainable alternative to synthetic plastics [14].

To date, no comprehensive research has clearly established the relationship between the structural properties of EVOH polymeric films and their mechanical performance. Understanding the size-scale-dependent properties of EVOH is critical for optimizing its application in food packaging. This study addresses this gap by investigating how ethylene content and blown film thickness in EVOH films influence key mechanical properties, including elongation at break, elastic modulus, and tensile strength. By exploring these factors, this research aims to provide a deeper understanding of the material's performance and guide its effective use in packaging applications.

2 | Experimental Section

2.1 | Materials

Three different EVOH pallets of 44 mol% EVAL E171B, 48 mol% EVAL G176B, and 27 mol% EVAL L171B, which will be referred to as Samples G, E, and L, were provided from EVAL manufactured by Kuraray Co. Ltd. Houston, TX.

2.2 | Preparation of EVOH Flexible Films

A Labtech Ultra Micro Film Blowing Line (model LUMF-150) single-screw extrusion extruder was utilized to produce films. The extruder featured a conical screw with an 18 mm diameter at the feed section, narrowing to 8 mm at the screw end, and an L:D ratio of 30:1. The screw speed was set to 80 rpm, and three extrusion speeds (4, 7, and 10 rpm) were applied via the tower Nip-roll Haul-off to achieve film thicknesses of 0.1, 0.05, and 0.03 mm. The extruder temperature was adjusted according to the melting points of three EVOH polymer samples: EVAL G176B (48%, melting temperature 157°C), EVAL E171B (42%, melting temperature 165°C), and EVAL L171B (27%, melting temperature 190°C). Film thickness was measured using a Mitutoyo 530-119 Vernier Caliper, with a range of 0–12″, an accuracy of ±0.0015″, and a resolution of 0.001″. These samples are referred to as G, E, and L throughout the study.

2.3 | Experimental Design

In this study, RSM was selected to identify the optimal conditions for variables, thickness, and EVOH mol%. RSM offers several advantages over traditional methods, including the need for fewer experiments, providing optimized parameters, and reducing time and costs [15–17]. Optimal design of experiments is highly versatile, making it suitable for various experimental needs [18]. Its flexible structure adapts to component limitations and irregular experimental areas. This method reduces overall variability in parameter estimates, accommodates irregularly shaped designs, and excludes areas from the design space, where measurements cannot be taken due to physical or operational constraints [19].

There are several types of optimality criteria [20]. D-optimality, for instance, chooses experimental runs that minimize the determinant of the variance–covariance matrix, thereby maximizing the information about parameter coefficients and designing factorial experiments to identify key process factors. A-optimality

focuses on minimizing the generalized variance of the parameter estimates for regression coefficients. G-optimality aims to minimize the maximum average prediction variance integral over the selected model [21, 22]. I-optimal designs excel by offering lower average prediction variance and more accurate factor effect estimates compared to other optimal designs. They are particularly beneficial for product and process optimization, enabling precise predictions and determination of factor settings to achieve desired outcomes [23].

In this research, the three response variables, including elongation at break, Y_1 (%), elastic modulus, Y_2 (MPa), and tensile strength, Y_3 (MPa), were determined by changing the independent variables, including EVOH mol% and thickness denoted as A and B, respectively. The I-optimal experimental design was executed for a total of 14 runs, and the design matrix developed using Design Expert Software is listed in Table 1.

To optimize the parameters and develop a prediction model using the I-optimal approach, a quadratic function was employed to establish the relationships between the variables (X_i) and the output responses (Y). The mathematical Equation (1) represents a quadratic polynomial that describes the relationship between dependent and independent variables, illustrating the optimization process used to predict the responses in this study.

$$Y_i = b_0 + b_1x_1 + b_2x_2 + b_{11}x_1^2 + b_{22}x_2^2 + + b_{12}x_1x_2 + \varepsilon \quad (1)$$

where Y_i is the predicted response, x_1 and x_2 are independent variables, b_0 is the offset term, b_1 and b_2 are linear effects, b_{11} and b_{22} are squared effects, and b_{12} is the interaction term. To evaluate the predictive accuracy of the mathematical equation, analysis of variance (ANOVA) was utilized. Several factors were considered to assess the statistical fitness of the model, including the determination coefficient (R^2), adjusted determination coefficient (R^2adj), F value, and P value. Additionally, 3-D graphical plots illustrated the individual and combined effects of the independent variables on the dependent variables.

2.4 | Tensile Properties

The films' mechanical properties were examined through tensile tests conducted with a Zwick Roell Z2.5 universal testing machine. The testing followed the ASTM D882-10 standard, using a 20 N ceramic load cell, and five samples from each batch were tested to ensure consistent results.

2.5 | Fourier Transform Infrared Spectroscopy

The Fourier transform infrared (FTIR) spectra of the polymer films were obtained using a Shimadzu IRTracer-100 spectrophotometer in transmittance mode over wavelengths ranging from 500 to 4000 cm^{-1} at a resolution of 4 cm^{-1}.

2.6 | Scanning Electron Microscopy

To analyze the fracture surfaces of the films after tensile testing, a Jeol-7200F FE SEM was used. The films were mounted on an SEM sample holder with the fractured surfaces facing upward for detailed examination. These samples were sputter-coated with gold/palladium to avoid char buildup.

TABLE 1 | Experimental runs from the I-optimal design and the respective responses based on actual and predicted values.

	Factor 1	Factor 2	Response 1	Response 2	Response 3
Run	A: EVOH mol%	B: Thickness (mm)	Elongation at break (%)	Elastic modulus (MPa)	Tensile strength (MPa)
1	0.44	0.05	15.352	2592.250	54.427
2	0.44	0.10	36.890	1124.016	27.138
3	0.27	0.05	37.911	2286.135	43.135
4	0.44	0.05	16.849	2703.308	52.875
5	0.48	0.03	28.352	3512.430	105.358
6	0.44	0.05	16.482	2663.523	53.432
7	0.27	0.03	9.358	2807.462	46.040
8	0.48	0.10	68.096	938.465	23.543
9	0.48	0.03	25.886	3363.191	109.258
10	0.44	0.10	35.983	1257.551	25.112
11	0.27	0.10	42.838	1267.560	24.564
12	0.44	0.05	15.583	2634.843	52.361
13	0.48	0.05	37.216	1940.690	60.181
14	0.44	0.03	6.386	2623.841	65.955

2.7 | Thermogravimetric Analysis

Thermogravimetric analysis (TGA) was carried out in a TA Q 500TGA. PSPW (15 mg) samples were heated from 30°C to 500°C at a heating rate of 10°C/min under a nitrogen atmosphere.

3 | Results and Discussion

3.1 | Optimal Design of Experiment and Data Analysis

Table 2 presents the mathematical equations that depict the relationships between the studied properties and the controlling parameters, along with the ANOVA results, including *P* value, *F* value, R^2, and Adj-R^2 for all three responses. Generally, film thickness and EVOH mol% directly influence the mechanical properties of the film. The I-optimal design results were used to develop a mathematical equation relating the studied factors to the responses, with statistical modeling conducted to maximize and evaluate the interaction effects between variables and responses.

As mentioned, a factor is considered to have a significant effect on the response when the *P* value is less than 0.01 [24] and R^2 represents the proportion of total variability explained by the regression model, measuring the extent of response variation accounted for by the variables. Notably, R^2 always increases with the addition of a new term, regardless of the term's statistical significance.

According to Table 2, for elongation at break, *P* values <0.0001 show the significance of the model. The elastic modulus equation also includes similar terms, showing strong significance and model fit ($R^2=0.9995$, adjusted $R^2=0.9992$). In addition, for tensile strength, the model shows high statistical significance (*P* values <0.0001) and strong predictive accuracy, with R^2 values of 0.9824 and 0.9714, indicating a reliable fit to the data. The ANOVA results indicate that most terms are significant (*P* values <0.0001), demonstrating that the model effectively captures the relationships between the factors and the responses.

3.1.1 | Effect of Thickness and EVOH Mol% on the Elongation at Break

Statistical modeling was conducted to enhance and investigate the interaction effects between the variables and responses using the I-optimal design (Table 2). The equation includes significant terms for A (EVOH mol%), B (thickness), and quadratic terms (A^2), with a high model fit indicated by $R^2=0.946$ and adjusted $R^2=0.912$. These terms have *P* values less than 0.01 and substantial *F* values of 14.410, 82.071, and 62.011, respectively, indicating the statistical significance of these factors in affecting elongation at break, with B having the most substantial impact (lowest *P* value and highest *F* value).

Figure 1a–d illustrates the relationship between two independent variables, EVOH mol% (A) and thickness (B), on elongation

TABLE 2 | Equations derived detailing the relationships between process parameters and the evaluated responses.

Response	Equation (actual factors)	*P*-value	*F*-value	R^2	Adj-R^2
Elongation at break	$(\text{Elongation at break})^{0.67} = +93.76482$	<0.0001	28.240	0.946	0.912
	$-557.02618*A$	$A=0.0053$	$A=14.410$		
	$+268.71401*B$	$B<0.0001$	$B=82.071$		
	$+67.10918*A*B$	$A^2<0.0001$	$A^2=62.011$		
	$+757.43327*A^2$				
	$-1424.58060*B^2$				
Elastic modulus	$(\text{Elastic modulus})^{-0.44} = +0.071181$	<0.0001	34.660	0.9995	0.9992
	$-0.23413*A$	$B<0.0001$	$B=107.540$		
	$-0.084311*B$				
	$+0.46224*A*B$				
	$+0.28455*A^2$				
	$+0.99713*B^2$				
Tensile strength	$(\text{Tensile strength})^{-0.86} = +0.050344$	<0.0001	89.22	0.982	0.971
	$-0.031383*A$	$A=0.0056$	$A=14.051$		
	$-0.29825*B$	$B<0.0001$	$B<242.610$		
	$+1.14379*A*B$	$AB=0.0087$	$AB=11.871$		
	$-0.11011*A^2$				
	$+2.73805*B^2$				

A: EVOH mol %, B: Thickness

at break as a response. Figure 1a shows the plot of predicted versus actual values. The even distribution of points along the diagonal indicates the model's reliability in making accurate predictions. Figure 1b illustrates the one-factor impact of EVOH ethylene content on elongation at break, emphasizing the quadratic term (A^2). Increasing ethylene content initially decreases elongation at break. However, beyond a certain point, further increases in ethylene content enhance flexibility and ductility, leading to a higher elongation at break and improved impact resistance. It can be concluded that at higher ethylene contents, the polymer chains gain more flexibility, allowing the material to stretch more before breaking, resulting in an increase in elongation at break. Thus, increased ethylene content initially reduces mechanical strength but eventually enhances flexibility and elongation at break. Also, the blue dashed lines on the graph represent the 95% confidence interval (CI) bands, indicating the range within which we can be 95% confident that the true mean response lies.

On the other hand, Figure 1c shows a nonlinear relationship between EVOH mol% and elongation at break. As EVOH mol% increases, elongation at break rises until reaching a peak, representing the optimal EVOH mol% for maximum tensile strength. The 3D response surface graph in Figure 1d highlights a specific region (indicated by the red-colored area), where the elongation at break is at its optimum. For instance, with an EVOH content of 48% and a thickness of 0.1 mm, the film achieves an elongation of 70%.

3.1.2 | Effect of Thickness and EVOH Mol% on the Elastic Modulus

The relation between thickness and EVOH mol% with the elastic modulus of the prepared films is summarized in Table 2. The model itself is highly significant, as indicated by a P value of <0.0001 and an F value of 34.66, demonstrating that the

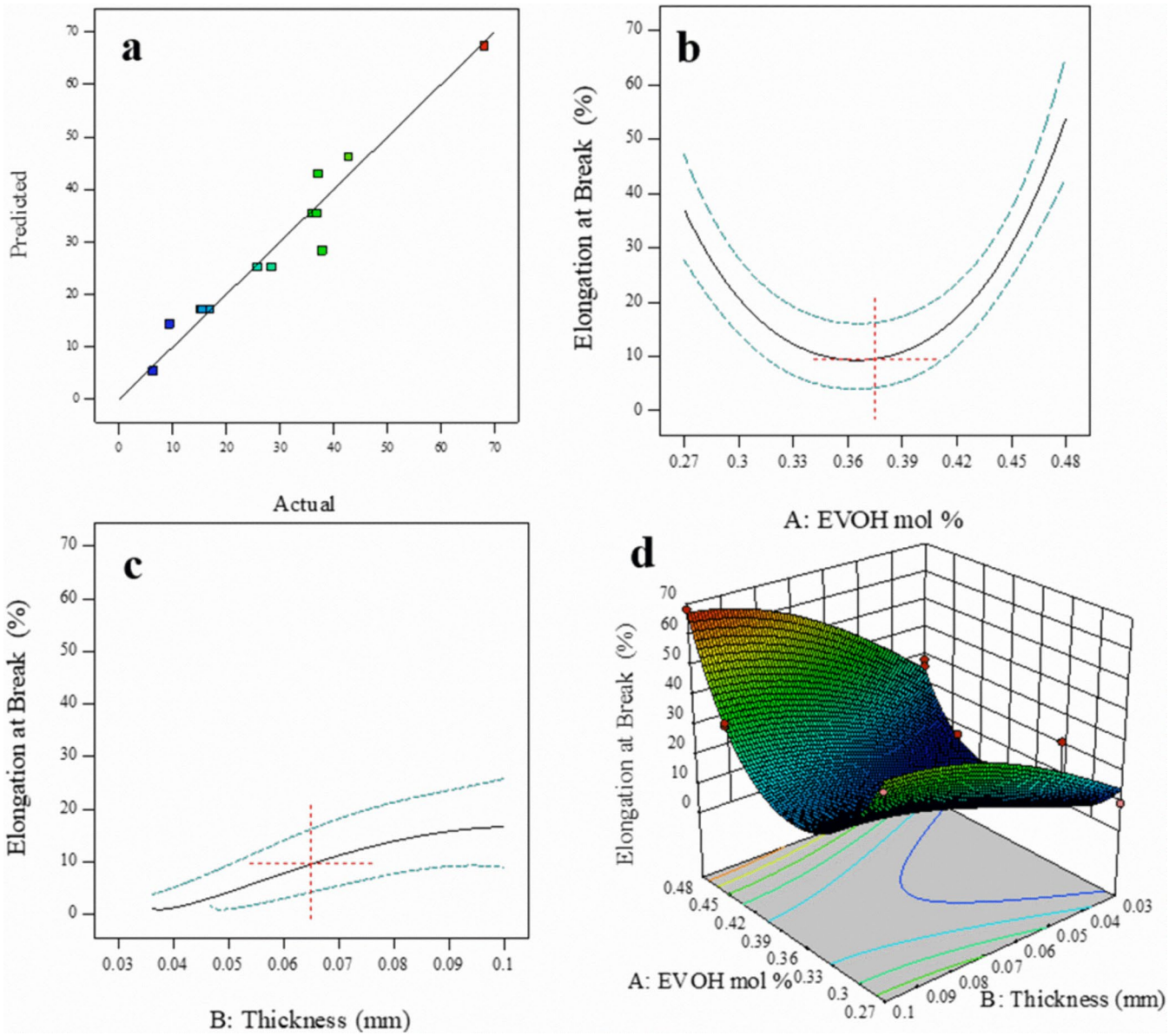

FIGURE 1 | (a) Predicted versus actual plot. (b) One-factor effect of EVOH mol% on elongation at break. (c) One-factor effect of thickness on elongation at break. (d) Effect of thickness and EVOH mol% on the elongation at break. [Color figure can be viewed at wileyonlinelibrary.com]

model explains a substantial portion of the variability in the data. Among the individual terms, thickness (B) is significant with a P value of <0.0001 and a high F value of 107.54, indicating a strong influence on the response variable. It indicates that the quadratic model can predict the relation between variables and responses, as shown in Figure 2a, which indicates that the distribution of points around the linear line in the predicted versus actual plot is homogeneous. According to Figure 2b, increasing EVOH mol% does not significantly change the elastic modulus. Conversely, thickness has a more profound impact on the elastic modulus, with a decrease in thickness leading to a sharp increase in elastic modulus. The same results can be seen in Figure 2d, which shows a single red region as the optimum elastic modulus, which takes place at a lower thickness.

3.1.3 | Effect of Thickness and EVOH Mol% on the Tensile Strength

The model depicting the relationship between tensile strength, thickness, and EVOH mol%, along with the corresponding ANOVA results, is shown in Table 2. The equation provided is quadratic, with a P value below 0.01, confirming its suitability for predicting the relationship between thickness, EVOH mol%, and tensile strength. Among the individual factors, B (thickness) has the most significant impact with an F value of 242.6112 and a P value <0.0001. Term A (EVOH mol%) also shows a significant effect (F value: 14.047, P value: 0.0056). The interaction term AB is significant (F value: 11.871, P value: 0.0087). The residual error is small, indicating that the model fits the data well. Furthermore, the values of R^2 and Adj-R^2 indicate that the

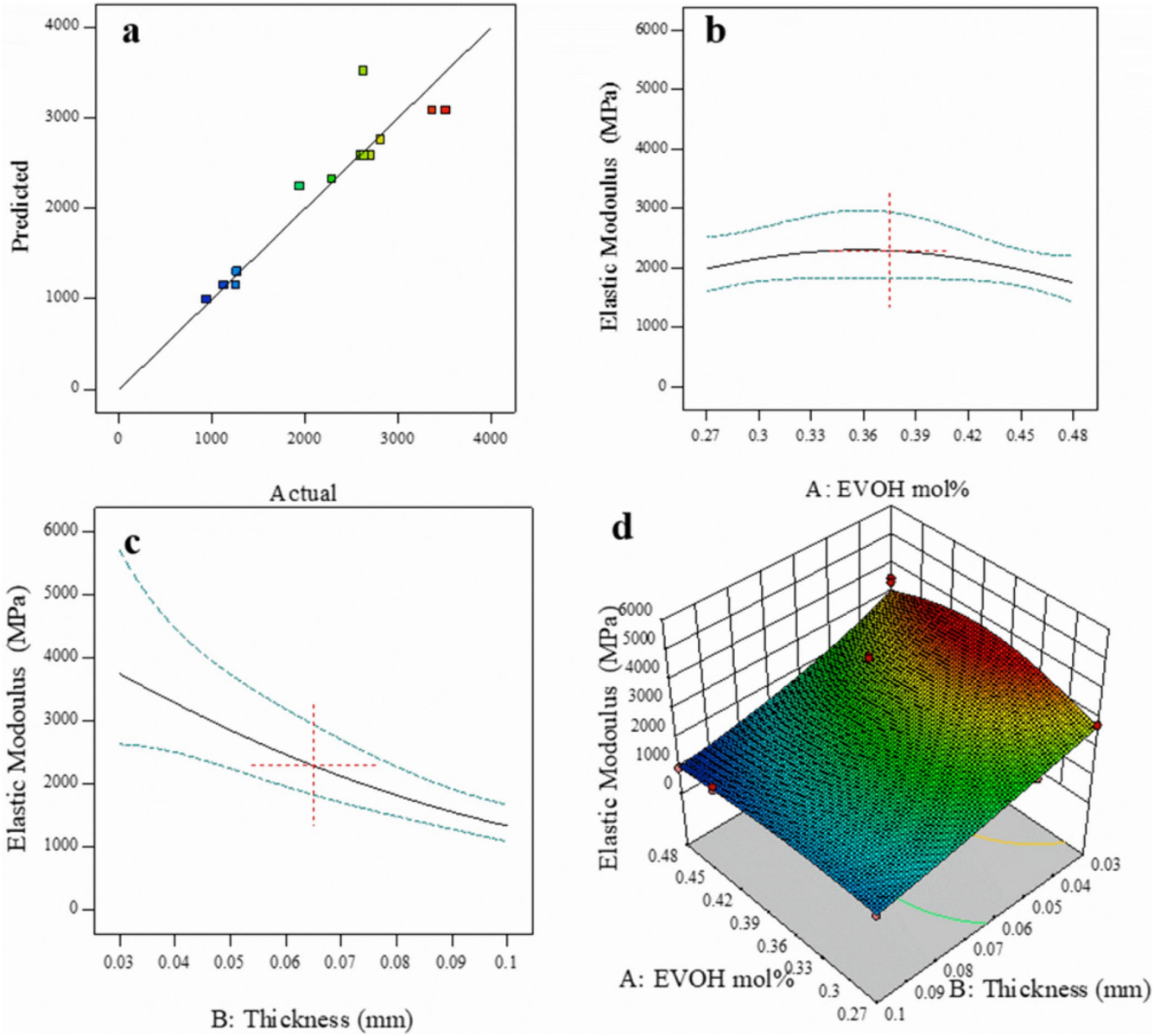

FIGURE 2 | (a) Predicted versus actual plot. (b) One-factor effect of EVOH mol% on elastic modulus. (c) One-factor effect of thickness on elastic modulus. (d) Effect of thickness and EVOH mol% on the elastic modulus. [Color figure can be viewed at wileyonlinelibrary.com]

model is in good agreement with the obtained results. Figure 3a shows a uniform distribution of points around the line. As can be seen in Figure 3b, the increasing trend of the curves suggests that as Thickness increases, the tensile strength decreases. On the other hand, Figure 3c shows a downward trend, suggesting that as the EVOH mol% increases, the response variable also increases. The 3D response surface graph in Figure 3d highlights the region where the tensile strength is at its optimal level (red-colored area).

3.2 | Optimization and Verification of the Models

The elongation at break, elastic modulus, and tensile strength were selected to be at their maximum possible values due to their importance in the packaging film industry. Based on the modeling results for EVOH mol%, thickness, and responses, the optimal solution was selected from seven calculated solutions, with the highest desirability value of 60.2% (Table 3). This optimal solution predicts achieving an elongation at break of 25.178, an elastic modulus of 3077.865, and a tensile strength of 97.444 for films, with 48% mol EVOH and 0.03 mm thickness.

TABLE 3 | Experimental validation of the optimal solution.

Thickness = 0.03 mm, EVOH mol% = 48% (optimal desirability = 60.2%)			
	Predicted	**Experimental**	**Error**
Elongation at break	25.178	27.119	7.15%
Elastic modulus	3077.865	3437.811	10.47%
Tensile strength	97.444	107.308	9.19%

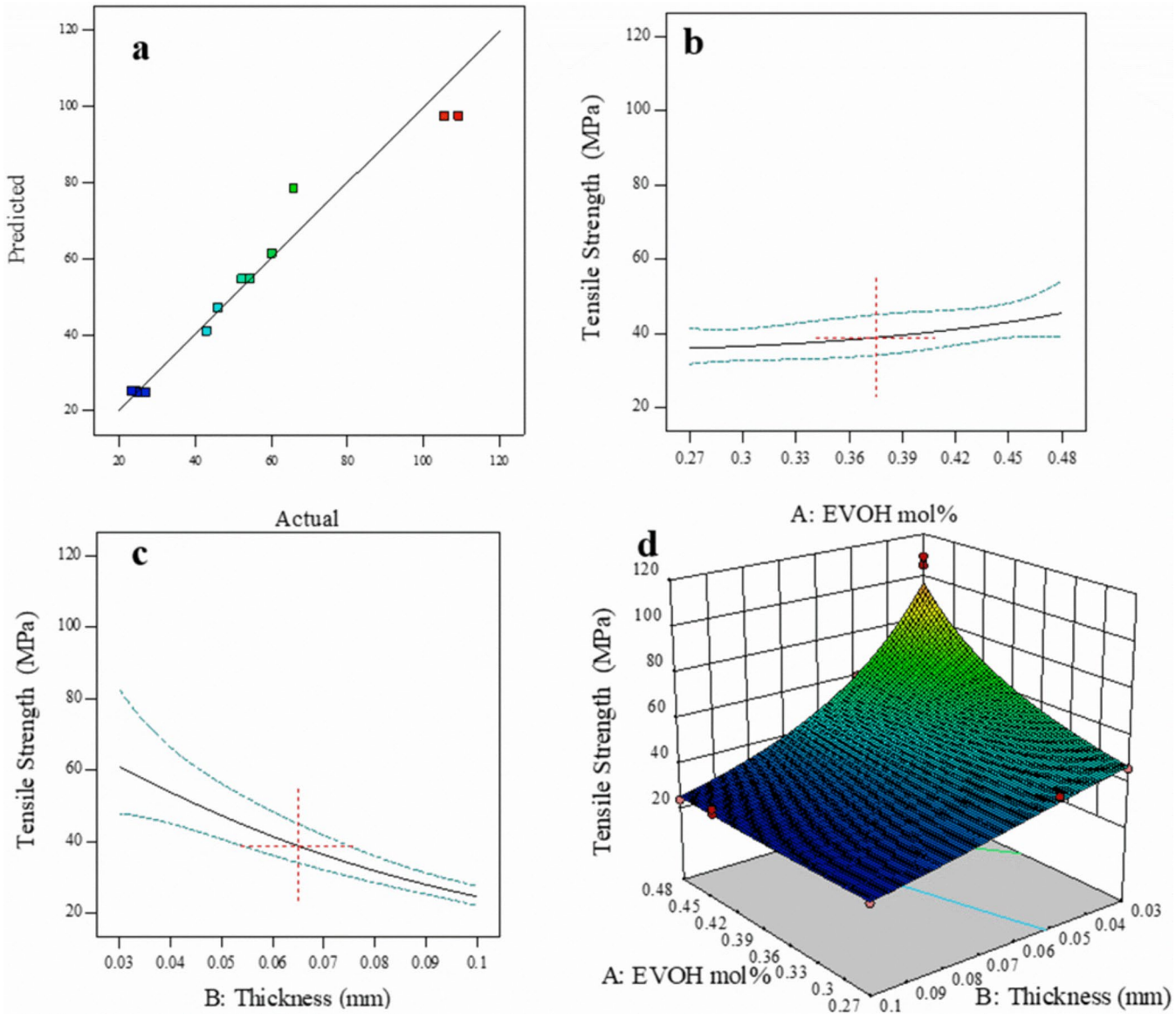

FIGURE 3 | (a) Predicted versus actual plot. (b) One-factor effect of EVOH mol% on tensile strength. (c) One-factor effect of thickness on tensile strength. (d) Effect of thickness and EVOH mol% tensile strength. [Color figure can be viewed at wileyonlinelibrary.com]

4 | Experimental Test Results

4.1 | FTIR Spectral Analysis

FTIR spectroscopy is an effective technique for analyzing the molecular structure of polymers and studying moisture sorption by detecting water-sensitive bonds. It is particularly useful for assessing penetrant/polymer interactions and transport properties in thin films, outperforming gravimetry in sensitivity and handling. However, research on the FTIR spectrum of water sorbed by EVOH copolymers and their blends remains limited [25, 26]. Figure 4a–c displays the FTIR spectra of selected EVOH films with varying thicknesses and types. All films exhibit characteristic absorption peaks at 2800–3000 cm^{-1} and 1300–1500 cm^{-1}, corresponding to —CH_2 stretching and —CH_3 deformation bands, respectively. Additionally, absorption bands near 3100–3600 cm^{-1} indicate the presence of —OH groups and bending vibration arround1300 cm^{-1} (C—H) and 1450 cm^{-1} (C—H). Despite these variations in ethylene content and thickness, there were no significant changes in the intensity or position of the characteristic peaks.

4.2 | TGA Analysis

While glass-transition temperature (T_g) primarily influences chain mobility, its effect is less dependent on film thickness. However, thinner films might exhibit thermal and mechanical inconsistencies during processing, which could indirectly affect T_g-related properties. EVOH films with higher ethylene content, which have lower crystallinity, may show reduced barrier performance, as observed in EVOH32, EVOH38, and EVOH44, which achieve crystallinity levels of 48%, 56%, and 60%, respectively [27]. In thinner films, this effect is amplified, as the amorphous regions dominate the structure and reduce the diffusion resistance. Therefore, EVOH's glass T_g and free volume are crucial to its barrier behavior. With a T_g between 50°C and 63°C, depending on ethylene content, EVOH maintains low chain mobility and excellent gas barrier properties at room temperature, outperforming materials like PE and PP, which have lower T_g values and higher permeability [27, 28]. The TGA in Figure 5 indicates that the thermal stability of EVOH films with different ethylene contents (48%, 42%, and 27%) and thicknesses (0.1, 0.05, and 0.03 mm) is consistent across all samples. All EVOH films had two-step degradation patterns, and there were no significant differences in the initial degradation temperature and weight loss of the samples. However, in all EVOH compositions, thinner films (0.03 mm) generally exhibit slightly higher degradation temperatures compared to thicker films (0.05 mm), likely due to improved heat dissipation and lower internal thermal buildup. This indicates that thinner films offer better thermal stability. For instance, in Sample G (48% ethylene), the degradation temperature increases from 378°C for the 0.05 mm film to 380°C for the 0.03 mm film. A similar trend is observed for Samples L (27%) and E (42%). In addition, films with higher ethylene content (G, 48%) degrade at lower temperatures compared to those with lower ethylene content (L, 27%). For example, the EVOH G pellet degrades around 360°C, whereas the L pellet degrades around 390°C, suggesting that higher ethylene content increases the amorphous regions, delaying thermal degradation.

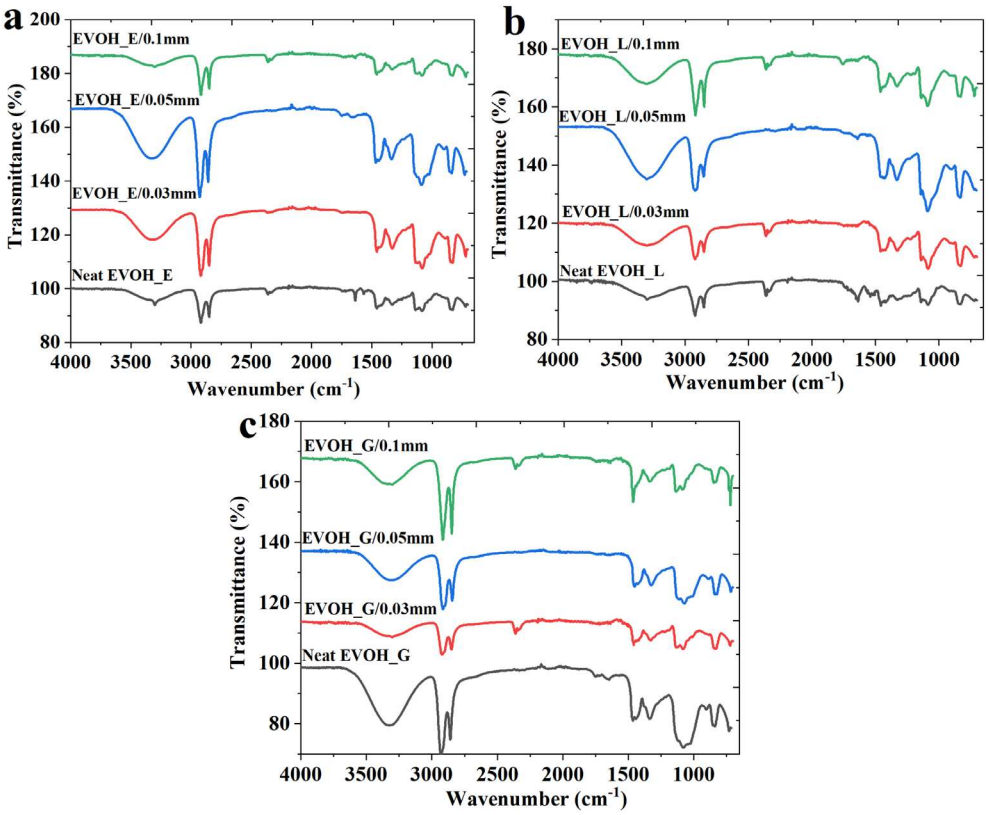

FIGURE 4 | FTIR spectra of EVOH films with varying ethylene contents and thicknesses: (a) Sample E (42% ethylene), (b) Sample L (27% ethylene), and (c) Sample G (48% ethylene). [Color figure can be viewed at wileyonlinelibrary.com]

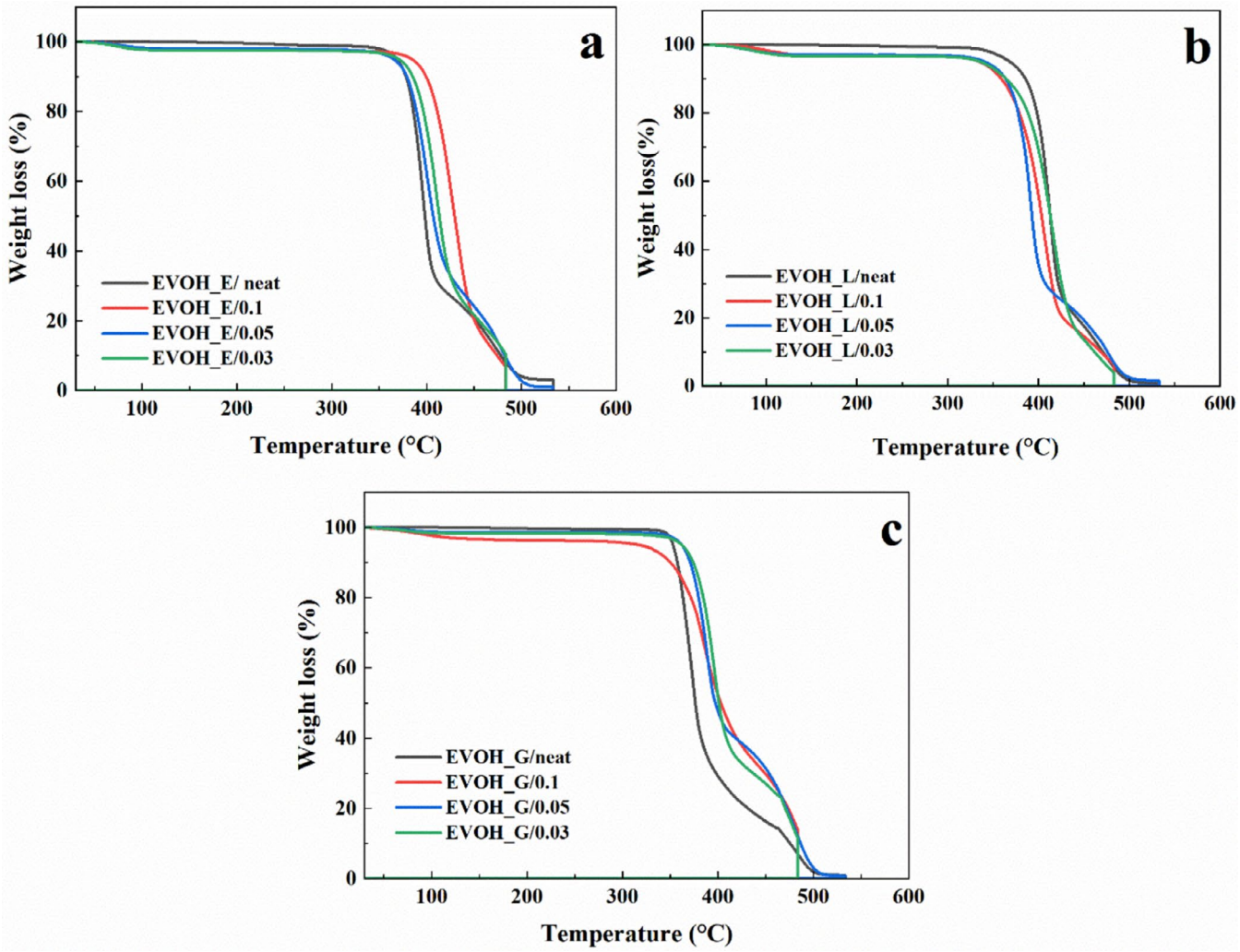

FIGURE 5 | TGA analysis of EVOH films with varying ethylene contents and thicknesses: (a) Sample E (42% ethylene), (b) Sample L (27% ethylene), and (c) Sample G (48% ethylene). [Color figure can be viewed at wileyonlinelibrary.com]

This indicates that higher ethylene content reduces thermal stability. Total weight loss is generally high across all samples, with some variation, and the thermal stability appears to be similar for all three compositions (48%, 42%, and 27%), with no significant differences observed in the TGA curves.

4.3 | Tensile Analysis

The ethylene content in EVOH copolymers is a critical determinant of their crystalline structure, degree of crystallinity, mechanical properties, and barrier performance. At high ethylene content (over 80 mol%), EVOH exhibits an orthorhombic crystal structure similar to polyethylene (PE), while intermediate compositions display a mix of orthorhombic and monoclinic structures with reduced crystallinity [12, 29]. Reducing the thickness of polymer layers in multilayer films can significantly impact their morphology and enhance their mechanical and barrier properties. In a study by Franco-Urquiza et al. the effects of strain rate, drawing temperature, and clay reinforcement on the mechanical behavior of EVOH and its composites were explored. The study found that low strain rates promote strain-induced crystallization and hardening, while high strain rates restrict molecular mobility, reducing these effects. Higher temperatures increased ductility but decreased stiffness and strength due to crystalline softening, with EVOH demonstrating high plasticity at 125°C. Clay reinforcement improved stiffness and strength by hindering molecular mobility but introduced microvoids due to filler–matrix decohesion. At elevated temperatures, clay's impact on ductility diminished because of EVOH's high molecular relaxation. The study concluded that optimizing strain rate, temperature, and clay content enhances EVOH's mechanical properties, making it suitable for applications requiring both strength and flexibility [30].

Figure 6 represents the stress–strain behavior of selected EVOH films, including the optimum film, at different thicknesses and mol% under tensile loading. As mentioned, the optimal conditions were chosen to give us the highest quantities of the considered responses, including elongation at break, elastic modulus, and tensile strength. The selection of the optimal point, Sample G at 0.03 mm thickness, was based on its ability to withstand high stress and strain, indicating a favorable balance of strength and flexibility. Figure 6b–d shows the tensile results of three EVOH mol% samples with the same thickness. In all these figures, Sample G exhibits the

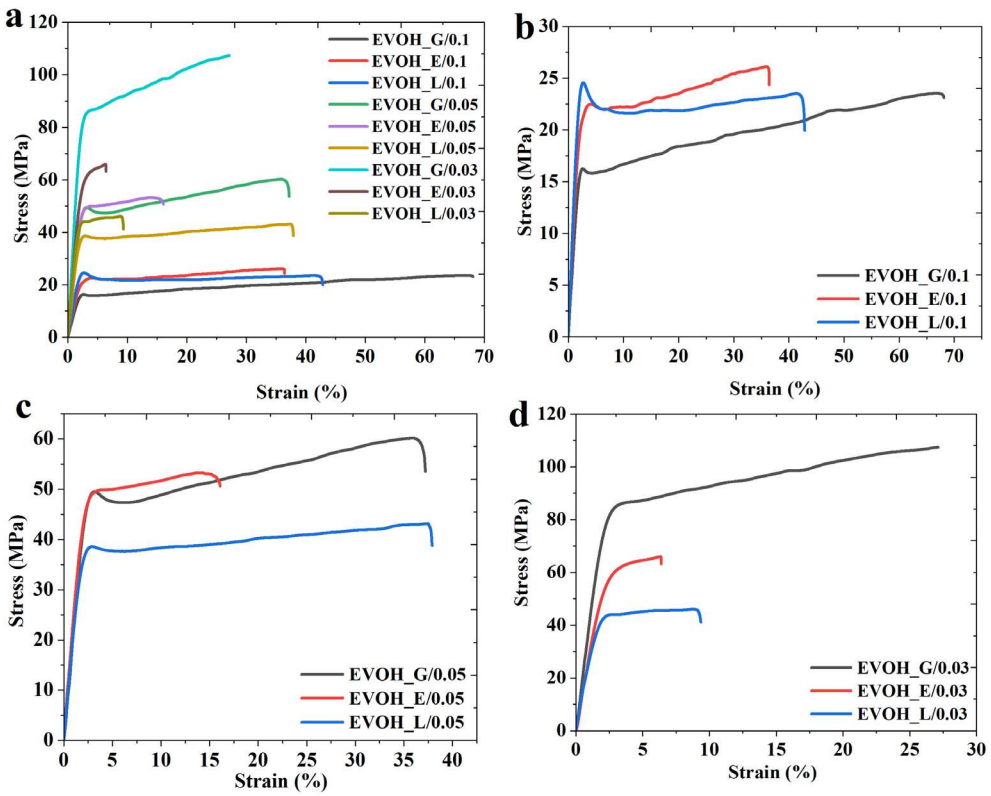

FIGURE 6 | Tensile analysis of EVOH films with varying ethylene contents and thicknesses: (a) selected samples, (b) sample with a thickness of 0.1 mm, (c) thickness of 0.05 mm, and (d) thickness of 0.03 mm. [Color figure can be viewed at wileyonlinelibrary.com]

highest elongation compared to other samples, which can be interpreted as the high ethylene content likely contributes to its enhanced mechanical properties, including both strength and ductility.

The mechanical behavior of EVOH films with varying ethylene contents and thicknesses can be explained by the balance between crystallinity, molecular orientation, and chain mobility. Figure 6b,c illustrates the tensile behavior of films each with a thickness of 0.1 and 0.05 mm, respectively. In Figure 6b, Sample G (48%), with its higher amorphous phase, shows high elongation but lower strength in thick films due to increased chain mobility, while thinner films exhibit both high elongation and strength due to improved molecular orientation. In contrast, Sample L (27%), with its higher crystallinity, demonstrates greater tensile strength in thick films but lower strength in thinner films due to restricted crystallization, though elongation remains slightly higher than in Sample E (42%). Figure 6d shows the tensile results of films with the same thickness of 0.03 mm. Sample G exhibits the highest tensile strength among the three polymers, with the stress reaching up to approximately 100 MPa before failure. It also shows a considerable amount of strain, indicating good ductility. However, as mentioned, in all figures, it can be seen that Sample E (42%) has lower elongation compared to Sample L (27%), which is in line with the data presented and the trend presented in Figure 1b. Sample L with 0.03 mm thickness shows the lowest tensile strength among the three samples (Figure 6b,c), reaching about 40 MPa. Similarly, a study conducted by Jansson and Thuvander highlights the significant influence of film thickness on the mechanical properties of starch films plasticized with glycerol. Films were prepared through solution-casting with varying thicknesses from 0.3 to 2.6 mm. Results showed that stiffness and tensile strength increased with thickness up to 1 mm, but decreased with further thickness. Strain at failure decreased with increasing thickness, indicating that thicker films allowed more molecular relaxation and orientation during drying, resulting in higher crystallinity. The study concluded that film thickness significantly affects the mechanical properties of starch films [31].

4.4 | SEM and Tensile Analysis

The fractured surfaces of the selected films with the same thickness of 0.03 mm were analyzed by SEM, as shown in Figure 7a–i. Figure 7a–c displays the SEM images of the fracture surfaces of the film extruded under these optimal conditions identified by the I-optimal method. The fracture surface of Sample G (48%) with a thickness of 0.03 mm was found to be relatively ductile combining significant strength with the ability to deform considerably before failure, which is also supported by the achieved results. The fracture surfaces display significant plastic deformation, rough and irregular fracture surfaces, and the presence of fibrils, all indicative of ductile fracture mechanisms. These observations align with the tensile stress–strain curves shown in Figure 6, where Sample G demonstrates high tensile strength and ductility. Figure 7d–f shows the fracture surface of the Sample E film. The fracture surface is smoother compared to the images of Sample G, and

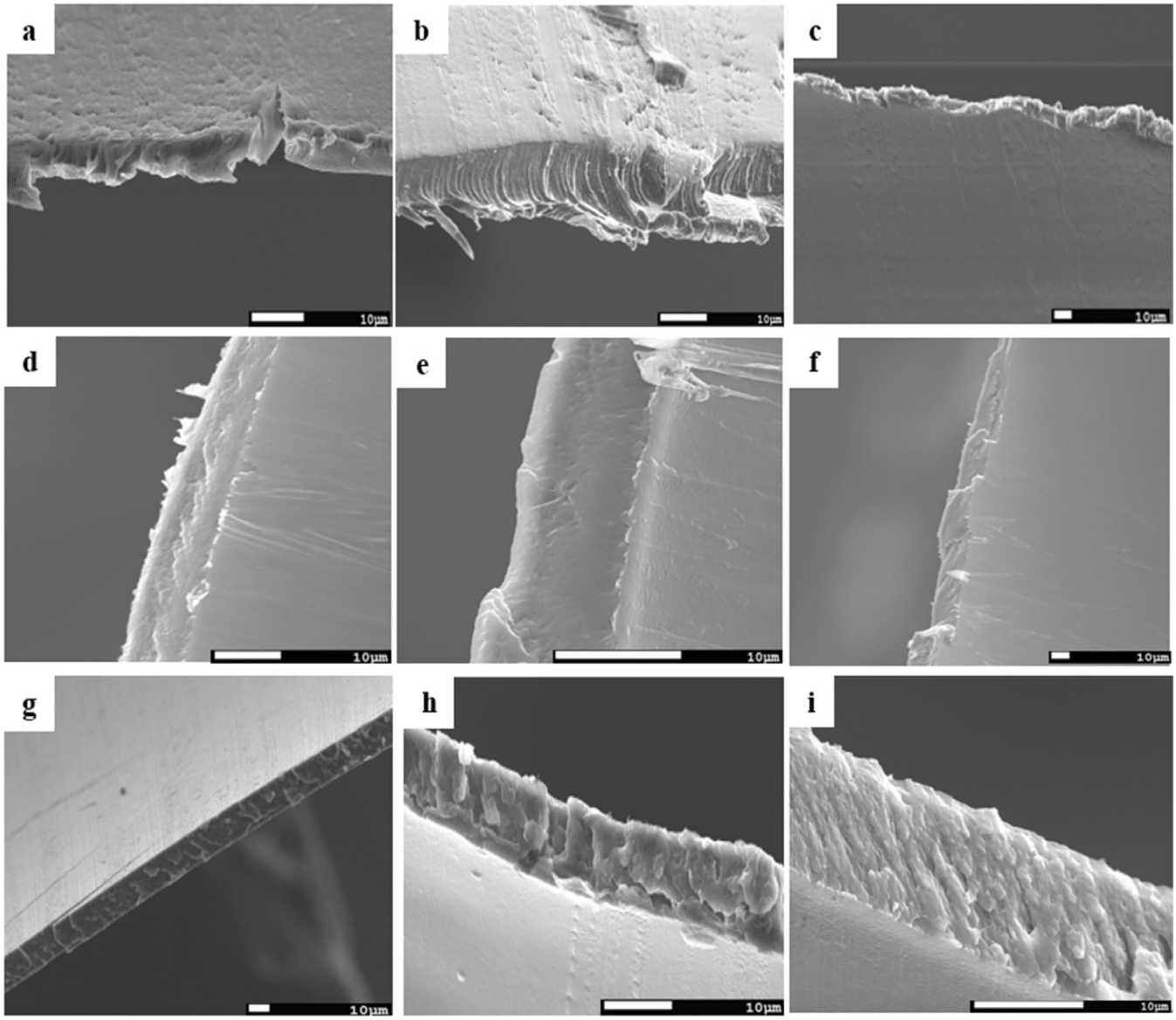

FIGURE 7 | SEM micrographs of the fractured surface films with a thickness of 0.03 mm: (a–c) Sample G (48%), (d–f) Sample L (42%), and (g–i) Sample E (0.27%).

the film has a uniform, homogenous, and smooth fractured surface, normally obtained for thermoplastic semicrystalline and well-processed polymeric matrices and copolymers. This characteristic highlights the good film-forming processability and properties of EVOH films during the selected process [32]. This aligns with tensile data, where Sample E showed lower tensile strength and ductility than Sample G, and it showed a quicker transition to failure, consistent with less plastic deformation, and the strain before failure is less than that of Sample G, indicating lower ductility. Figure 7g–i shows the SEM of the fracture surface of Sample L (27%) with a thickness of 0.03 mm. The fracture surface displays significant roughness and irregularities with many small ridges and valleys, suggesting some degree of plastic deformation before failure. This sample is less stiff, strong, and ductile compared to the previous one. In contrast, the 48% EVOH film's fracture surfaces exhibit significant plastic deformation, with rough, fibrous features, consistent with a tougher and more ductile material.

5 | Conclusion

This study highlights the impact of ethylene content and film thickness on the mechanical and thermal properties of EVOH films. Using mathematical modeling and RSM, the optimal conditions for achieving superior mechanical properties were identified. An EVOH film with 48% ethylene content and a thickness of 0.03 mm was identified as the optimal configuration, with experimental results closely matching the model's predictions. The quadratic model, validated by high R^2 values and supported by ANOVA, predicted the values of 25.178% for elongation at break, 3077.865 MPa for elastic modulus, and 97.444 MPa for tensile strength. Under optimal conditions, the achieved values were 27.119% for elongation at break, 3437.811 MPa for elastic modulus, and 107.308 MPa for tensile strength. The discrepancies between the predicted and experimental values were within 10%, demonstrating the accuracy of the model. Mechanical analysis revealed that films with higher ethylene content (G,

48%) exhibited exceptional elongation and ductility in thinner configurations due to enhanced molecular orientation, while thicker films displayed reduced tensile strength owing to increased chain mobility in the amorphous regions. Conversely, lower ethylene content (L, 27%) promoted higher crystallinity, resulting in improved tensile strength in thicker films but reduced strength in thinner films, where crystallinity was less dominant. Moderate elongation was observed in all cases for L, maintaining values between those of G and E.

Thermal analysis (TGA) demonstrated consistent two-step degradation patterns across all EVOH compositions. Thinner films (0.03 mm) showed slightly higher degradation temperatures, attributed to improved heat dissipation and reduced thermal stress, highlighting their superior thermal stability. However, higher ethylene content was associated with lower thermal stability, as evidenced by earlier degradation onset due to the dominance of amorphous regions. FTIR characterization confirmed uniform transmittance trends across all samples, while the SEM analysis of the optimal film's fracture surface revealed fibrous structures, indicative of significant plastic deformation and correlating with superior mechanical properties. This study highlights the influence of ethylene content and film thickness in optimizing the mechanical properties and performance of EVOH films, offering valuable insights for the development of high-performance EVOH films tailored for food packaging and other industrial applications requiring enhanced functionality, durability, and sustainability.

Author Contributions

Kowsar Rezvanian: conceptualization (equal), data curation (equal), formal analysis (lead), writing – original draft (lead). **Radhika Panickar:** formal analysis (equal), writing – review and editing (equal). **Faruk Soso:** writing – review and editing (supporting). **Vijaya Rangari:** conceptualization (equal), data curation (equal), funding acquisition (lead), supervision (lead), writing – review and editing (lead).

Acknowledgments

The authors would like to acknowledge the financial support from the NSF-CREST #1735971 and NSF-EFMA # 2132093.

Conflicts of Interest

The authors declare no conflicts of interest.

Data Availability Statement

The data that support the findings of this study are available from the corresponding author upon reasonable request.

References

1. F. Johansson and A. Leufven, "Food Packaging Polymer Films as Aroma Vapor Barriers at Different Relative Humidities," *Journal of Food Science* 59, no. 6 (1994): 1328–1331.

2. C. Ge and J. Popham, "A Review and Evaluation of Prediction Models of Gas Permeation for a Blended Flexible Packaging Film," *Packaging Technology and Science* 29, no. 4–5 (2016): 247–262.

3. J. Lagarón, E. Giménez, R. Gavara, and J. Saura, "Study of the Influence of Water Sorption in Pure Components and Binary Blends of High Barrier Ethylene–Vinyl Alcohol Copolymer and Amorphous Polyamide and Nylon-Containing Ionomer," *Polymer* 42, no. 23 (2001): 9531–9540, https://doi.org/10.1016/S0032-3861(01)00496-7.

4. S. Aucejo, R. Catala, and R. Gavara, "Interactions Between Water and EVOH Food Packaging Films/Interacciones Entre el AGUA y Películas de EVOH Para el Envasado de Alimentos," *Food Science and Technology International* 6 (2000): 159–164.

5. C. Maes, W. Luyten, G. Herremans, R. Peeters, R. Carleer, and M. Buntinx, "Recent Updates on the Barrier Properties of Ethylene Vinyl Alcohol Copolymer (EVOH): A Review," *Polymer Reviews* 58, no. 2 (2018): 209–246.

6. M. Buntinx, G. Willems, G. Knockaert, et al., "Evaluation of the Thickness and Oxygen Transmission Rate Before and After Thermoforming Mono- and Multi-Layer Sheets Into Trays With Variable Depth," *Polymers* 6, no. 12 (2014): 3019–3043, https://doi.org/10.3390/polym6123019.

7. A. R. Ajitha, M. K. Aswathi, H. J. Maria, J. Izdebska, and S. Thomas, "Multilayer Polymer Films," in *Multicomponent Polymeric Materials*, ed. J. Izdebska and S. Thomas (Elsevier, 2016), 229–258.

8. P. S. Alexopoulos and T. C. O'Sullivan, "Mechanical Properties of Thin Films," *Annual Review of Materials Science* 20 (1990): 391–420.

9. S. Cholтyssek, R. Adhikari, V. Seydewitz, G. H. Michler, E. Baer, and A. Hiltner, "Evaluation of Morphology and Deformation Micromechanisms in Multilayered PP/PS Films: An Electron Microscopy Study," *Macromolecular Symposia* 294, no. 1 (2010): 33–44.

10. M. Erber, M. Tress, E. U. Mapesa, et al., "Glassy Dynamics and Glass Transition in Thin Polymer Layers of PMMA Deposited on Different Substrates," *Macromolecules* 43 (2010): 7729–7733.

11. A. Serghei and F. Kremer, *Characterization of Polymer Surfaces and Thin Films*, vol. 132, ed. K. Grundke, M. Stamm, and H.-J. Adler (Springer, 2006), 33.

12. L. Cabedo, J. M. Lagarón, D. Cava, J. J. Saura, and E. Giménez, "The Effect of Ethylene Content on the Interaction Between Ethylene-Vinyl Alcohol Copolymers and Water—II: Influence of Water Sorption on the Mechanical Properties of EVOH Copolymers," *Polymer Testing* 25, no. 7 (2006): 860–867.

13. M. Rouhi, S. H. Razavi, and S. M. Mousavi, "Optimization of Crosslinked Poly(Vinyl Alcohol) Nanocomposite Films for Mechanical Properties," *Materials Science and Engineering: C* 71 (2017): 1052–1063.

14. K. D. Tafa, N. Satheesh, and W. Abera, "Mechanical Properties of Tef Starch-Based Edible Films: Development and Process Optimization," *Heliyon* 9, no. 2 (2023): e13160.

15. O. O. Olabinjo, "Response Surface Techniques as an Inevitable Tool in Optimization Process," in *Response Surface Methods—Theory, Applications, and Optimization Techniques* (IntechOpen, 2024).

16. J. Antony, *Design of Experiments for Engineers and Scientists* (Elsevier, 2023).

17. K. Rezvanian, "Optimizing Process Variables and Type in a Sweet Potato Starch Syrup: A Response Surface Methodology Approach," (2023), Doctoral Dissertation, Tuskegee University.

18. P. Goos and B. Jones, *Optimal Design of Experiments: A Case Study Approach* (John Wiley & Sons, 2011).

19. D. C. Montgomery, *Design and Analysis of Experiments* (John Wiley & Sons, 2017).

20. W. Ahmed and M. J. Jackson, *Emerging Nanotechnologies for Manufacturing* (William Andrew, 2014).

21. R. H. Myers, *Response Surface Methodology (RSM): Process and Product Optimization Using Designed Experiments* (Wiley, 2002), 489–492.

22. R. H. Myers, D. C. Montgomery, and C. M. Anderson-Cook, *Response Surface Methodology: Process and Product Optimization Using Designed Experiments* (John Wiley & Sons, 2016).

23. K. Van Brantegem, A. Strouwen, and P. Goos, "D- and I-Optimal Design of Multi-Factor Industrial Experiments With Ordinal Outcomes," *Chemometrics and Intelligent Laboratory Systems* 221 (2022): 104463.

24. K. Rezvanian, S. Jafarinejad, and A. C. Bovell-Benjamin, "A Review on Sweet Potato Syrup Production Process: Effective Parameters and Syrup Properties," *Pro* 11 (2023): 3280.

25. A. López-Rubio, J. M. Lagaron, E. Giménez, et al., "Morphological Alterations Induced by Temperature and Humidity in Ethylene–Vinyl Alcohol Copolymers," *Macromolecules* 36, no. 25 (2003): 9467–9476.

26. R. Y. Mahmood, A. A. Kareem, A. R. Polu, et al., "Structural, Electrical, and Electrochemical Investigations on Cu^{2+} Ion–Conducting PVA/HPMC-Based Blend Solid Polymer Electrolytes," *Ionics* 30 (2024): 7061–7070.

27. K. K. Mokwena and J. Tang, "Ethylene Vinyl Alcohol: A Review of Barrier Properties for Packaging Shelf Stable Foods," *Critical Reviews in Food Science and Nutrition* 52 (2012): 640–650.

28. S. M. Aharoni, "Increased Glass Transition Temperature in Motionally Constrained Semicrystalline Polymers," *Polymer Advances in Technology* 9 (1998): 169–201.

29. N. Artzi, "Why Nano-Composites Are in? A Glimpse Into Polymer-Based Nanocomposites," *Reviews in Chemical Engineering* 21 (2005): 307–345.

30. E. A. Franco-Urquiza, J. Gámez-Pérez, J. C. Velázquez-Infante, O. Santana, A. M. Benasat, and M. L. Maspoch, "Effect of the Strain Rate and Drawing Temperature on the Mechanical Behavior of EVOH and EVOH Composites," *Advances in Polymer Technology* 32, no. S1 (2012): E287–E296.

31. A. Jansson and F. Thuvander, "Influence of Thickness on the Mechanical Properties for Starch Films," *Carbohydrate Polymers* 56 (2004): 499–503.

32. E. Fortunati, F. Luzi, L. Dugo, et al., "Effect of Hydroxytyrosol Methyl Carbonate on the Thermal, Migration and Antioxidant Properties ofPVA-Based Films for Active Food Packaging," *Polymer International* 65 (2016): 872–882.